



# City Research Online

## City St George's, University of London

**Citation:** Santos, E., Ferreira, F. P. V., Martins, C. H. & Tsavdaridis, K. (2024). Finite Element Analysis of Steel-Concrete Composite Beams with Elliptically-Based Web Openings. Paper presented at the International Conference on Steel and Aluminium Structures (ICSAS 2024), 5-7 Jun 2024, Rio de Janeiro, Brazil.

This is the published version of the paper.

This version of the publication may differ from the final published version. To cite this item please consult the publisher's version.

**Permanent repository link:** <https://openaccess.city.ac.uk/id/eprint/33098/>

**Copyright and Reuse:** Copyright and Moral Rights remain with the author(s) and/or copyright holders. Copies of full items can be used for personal research or study, educational, or not-for-profit purposes without prior permission or charge, unless otherwise indicated, provided that the authors, title and full bibliographic details are credited, a hyperlink and/or URL is given for the original metadata page and the content is not changed in any way. For full details of reuse please refer to [City Research Online policy](#).

# FINITE ELEMENT ANALYSIS OF STEEL-CONCRETE COMPOSITE BEAM WITH ELLIPTICALLY-BASED WEB OPENINGS

**Eduardo V. SANTOS<sup>a</sup>, Felipe P. V. FERREIRA<sup>b</sup>, Carlos H. MARTINS<sup>a</sup> and  
Konstantinos D. TSAVDARIDIS<sup>c</sup>**

<sup>a</sup> Department of Civil Engineering, State University of Maringá, Av. Colombo n° 5790, Maringá, Paraná, Brazil  
Emails: eduardo.vedovetto@ifpr.edu.br, chmartins@uem.br

<sup>b</sup> Federal University of Uberlândia, Faculty of Civil Engineering – Campus Santa Mônica, Uberlândia, Minas  
Gerais, Brazil  
Email: fpvferreira@ufu.br

<sup>c</sup> Department of Civil Engineering, School of Mathematics, Computer and Engineering, City, University of  
London, Northampton Square, EC1V 0HB, London UK  
Email: konstantinos.tsavdaridis@city.ac.uk

**Keywords:** Steel-concrete composite beams; Elliptically-based web openings; Web-post buckling, Finite element method.

**Abstract.** *The use of steel-concrete composite beams with web openings becomes an advantageous tool used to reduce the height of the floor, as the web openings allow the integration of hydraulic and electrical services. This study aims to investigate the web-post buckling resistance of steel-concrete composite beams with elliptically-based web openings. A finite element model is developed to predict the behavior of steel-concrete composite beams with elliptical-base openings, considering experimental analyses. The numerical simulations are processed in two steps: buckling and post-buckling analyses. A parametric study is performed based on the geometric parameters of the openings, as well as the spacing between them. Increasing the slenderness of the web tends to change the failure mode, changing from web local buckling to web-post buckling, where the presence of the concrete slab and the elliptically-based openings contribute to the resistant capacity of the composite cellular beams.*

## 1 INTRODUCTION

The search for more efficient structures, such as steel-concrete composite beams, has increased in the civil construction, mainly due to the potential for reducing the structure's own weight, eliminating the need for formwork and shoring, and achieving faster construction speeds [1]. However, even with the increase in the cross-sectional area enhancing the flexural stiffness, the presence of openings makes steel beams susceptible to lateral-torsional buckling, web distortion, the formation of the Vierendeel mechanism (VM), web-post buckling (WPB), web local buckling, web-post rupture, or even a combination of buckling modes. Furthermore, the failure of the concrete slab combines with the failure of the steel beams, along with Vierendeel mechanism (VM) and web-post buckling (WPB) [1-5]. Regarding the behavior of steel beams with elliptically-based web openings, one can refer to the experimental and analytical study by Tsavdaridis and D'mello [6]. In this study, two cellular beams and four beams with novel web opening shapes were tested to investigate the failure mode. The web-

post resistance was the main failure to be investigated. The authors concluded that elliptically-based web openings had shown better stress distribution and greater resistance to horizontal shear stresses in comparison with circular web openings. Steel beams with such non-standardized openings were patented (GB 2492176) [7] by the authors and inventors Tsavdaridis and D'mello [8], with the key geometric parameters of the opening being highlighted. These parameters include the presence of a radius ( $R$ ) at the upper and lower positions of the opening, the opening width ( $w$ ), the spacing between the centers of the openings ( $s$ ), the opening height ( $d_o$ ), and the width of the web-post ( $b_w$ ), Figure 1.

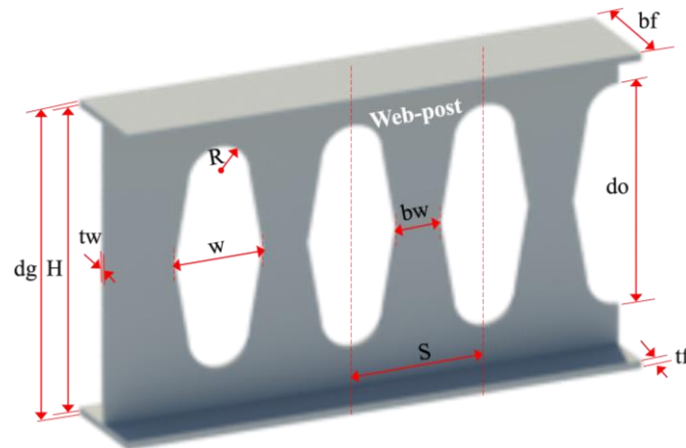


Figure 1: Geometric parameters for elliptical opening

Furthermore, Ferreira *et al.* [9] investigated the influence of geometric parameters on the resistance capacity to web-post buckling for steel beams with non-standardized elliptically-based web openings. Shamass *et al.* [10] proposed an Artificial Neural Network (ANN) model to determine the web-post resistance and failure mode of steel beams with elliptically web openings. Ferreira *et al.* [11] incorporated high-strength steels into the web-post buckling resistance, based on the truss model according to EN 1993-1-1 [12]. However, when it comes to composite beams with elliptically-based web openings, the literature lacks sufficient studies. Therefore, the present study aims to investigate the web-post buckling resistance of steel-concrete composite beams with elliptically-based web openings via finite element method. The effects of varying elliptically-based web openings on web-post behavior and the overall performance of steel-concrete composite beams were evaluated. The ABAQUS 6.14 software was used for modelling, conducting numerical analyses in two steps: buckling analysis, estimating the critical load, and post-buckling analysis.

## 2 FINITE ELEMENT ANALYSIS

The modeling was conducted using ABAQUS 6.14 software and analyzed in two stages: buckling and post-buckling analyses. The imperfection factor adopted was  $H/500$ , according to Panedpojaman *et al.* [13]. Nominal strength values for S355 steel were employed. Concerning the elastic behavior of the steel and connectors, a Young's Modulus of 200 GPa and a Poisson's ratio of 0.3 were used. For the plastic behavior of the steel, the quadri-linear model proposed by Yun and Gardner [14] was applied. A bi-linear model with hardening was used in shear connector, as per Araújo *et al.* [15]. For the concrete slabs, the concrete damage plasticity (CDP) model was employed, by using the concrete in compression model, according to the Model Code 2010 [16]. For concrete in tension, the model proposed by Hordijk [17] was used. According to the studies by Ferreira *et al.* [18], Ferreira, Martins, and De Nardin [1] and Ferreira *et al.* [2]. The mesh used for the steel cellular beams consists of shell elements (S4R),

quadrilateral with four nodes and reduced integration, with a free configuration and an average element size of 10 mm. The mesh for the concrete slab comprises hexahedral elements of type C3D8R, with an average size of 30 mm. The shear connectors and the actuator also have hexahedral elements of type C3D8R, with mesh discretization of 4 mm and 20 mm, respectively.

## 2.1 Steel beam models with elliptically-based openings

Two cellular beams (A1 and B1), a beam with a circular opening and circular web stiffener (A2), and two beams with elliptically-based openings (B2 and B3) were considered, all tested by Tsavdaridis and D'mello [6]. At the bottom of the stiffener in one end, vertical and longitudinal displacements are restrained ( $U_y = U_z = 0$ ). The analysis is performed with load control and the arc-length method is employed to capture the buckling behaviour. At the bottom of the stiffener in the other end, only the vertical displacement is restrained ( $U_y = 0$ ). At both ends, in the region of the stiffeners, lateral displacement and the rotation around the longitudinal axis are restrained at four points ( $U_x = U_z = 0$ ). The load-vertical displacement curves (Figure 2) obtained from the finite element models were compared with the curves from the experimental tests on steel beams with openings by Tsavdaridis and D'mello [6], aiming to validate the numerical models.

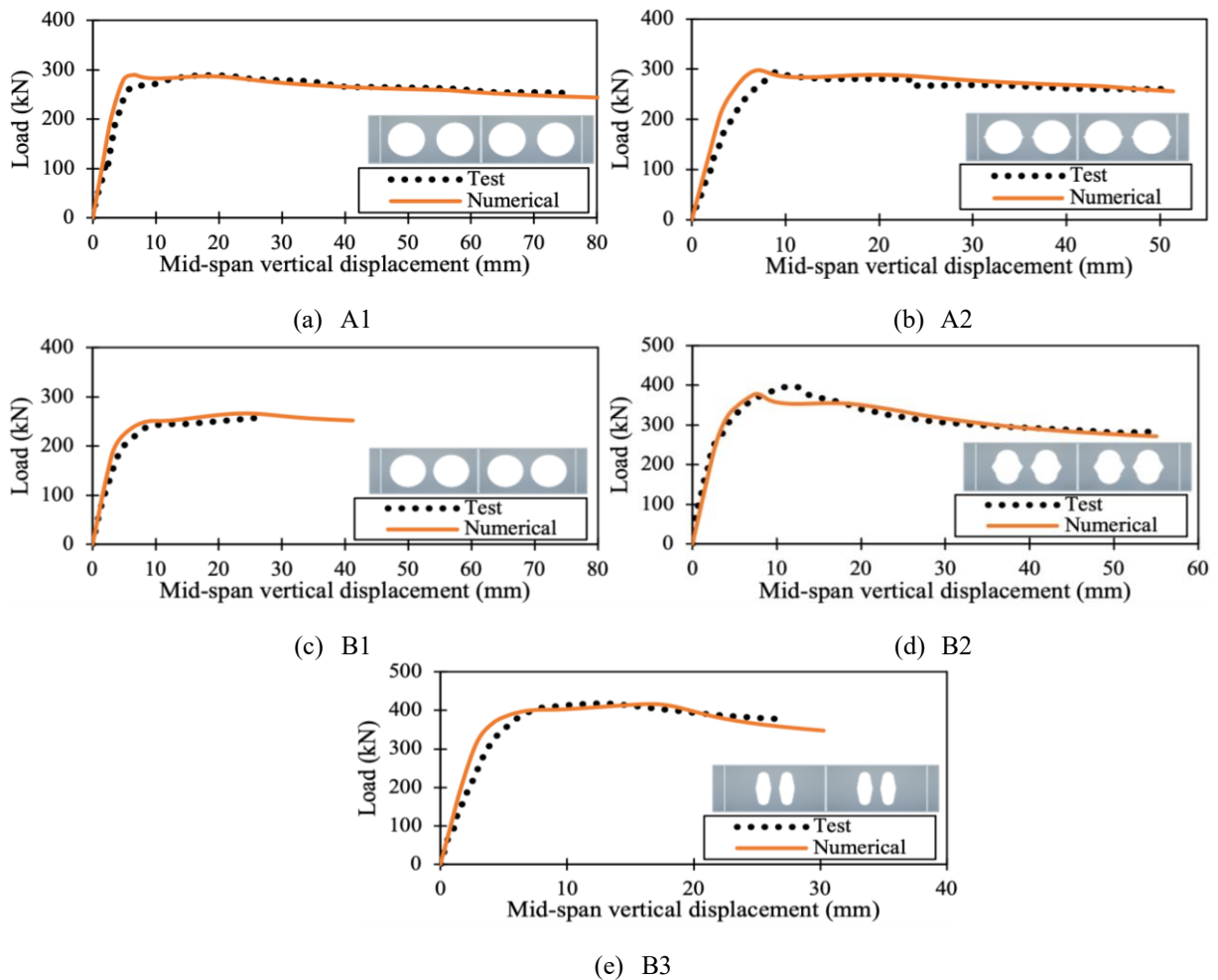


Figure 2: Validation results of models A and B, load-vertical displacement curves

## 2.2 Steel-concrete composite cellular beam models

Four steel-concrete composite cellular beams were considered. Two beams tested by Nadjai *et al.* [19], referred to in this study as CCB1 and CCB2, while beams CCB3 and CCB4 correspond to models tested by Müller *et al.* [20]. The composite cellular beam models were treated as simply supported and represented only by half of the structure, employing the methodology of longitudinal symmetry, the vertical displacement ( $U_y = 0$ ) and the lateral displacement on the concrete slab ( $U_x = 0$ ) were restrained on the support. In the middle of the span, symmetry was considered ( $U_z = UR_x = UR_y = 0$ ).

For models CCB1 and CCB2, a displacement ( $U$ ) was applied at the actuators located on the concrete slab. For models CCB3 and CCB4, a load ( $P$ ) was applied at the actuators located on the concrete slab. The interaction between the elements used in the modeling considered the normal/tangential behavior between the contact surfaces: steel cellular beam-concrete slab and slab-connector, with Coulomb friction values of 0.3 and 0.2, respectively [2]. The load-vertical displacement curves obtained from the finite element models for steel-concrete composite cellular beams (CCBs) were compared with the curve obtained in the experimental test (Figure 3) to calibrate the models for the parametric study.

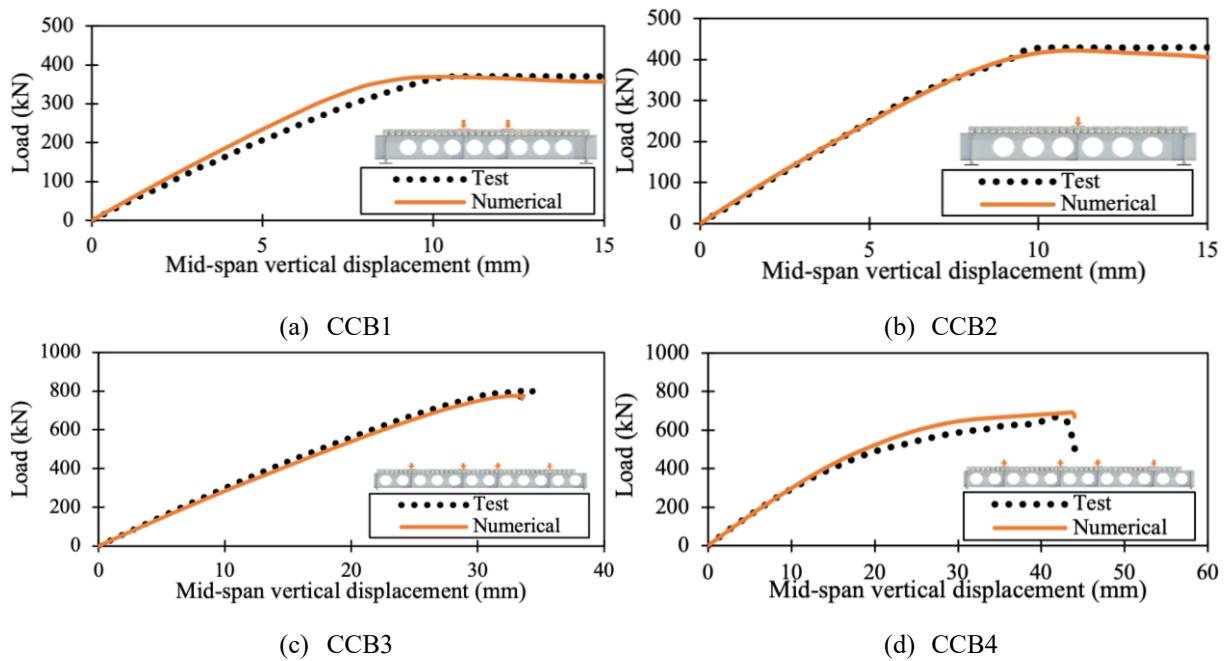


Figure 3: Validation results of the CCB models, load-vertical displacement curves

## 2.3 Parametric study

Once the numerical model of the composite beam is validated, the next step was the development of a parametric study (Figure 4). Three structural conditions were analyzed based on the structural and loading configuration of the CCB1, CCB2, and CCB3 models for the ratio  $d_o/H$  of 0.65, referred to as groups GCCB1, GCCB2, and GCCB3. This resulted in a total of 45 finite element models.

Variations were made to the opening radius ( $R$ ), opening width ( $w$ ), and web width ( $b_w$ ) at the following ratios:

1. The ratios  $b_w/d_o$  range from 0.2-0.3-0.4-0.5 to 0.60;
2. The ratios  $R/d_o$  range from 0.10-0.15-0.20-0.25 to 0.30;
3. The ratios  $w/d_o$  range from 0.25-0.35-0.45, 0.55 to 0.65;

4. Steel concrete composite beams with elliptically-based web openings are simply supported. GCCB1 beams were subjected to two point loads, while GCCB2 beams were subjected to a centered load. The GCCB3 group, on the other hand, was subjected to four point loads;

5. Both supports and load application points were reinforced with stiffeners of the same web thickness ( $t_w$ );

6. The end-post width should not be less than the width of the others web-posts dimensions ( $b_w$ );

7. The dimensions of the headed stud shear connector are 19x120mm for GCCB1 and GCCB2 reference models, and 19x100mm for GCCB3 reference models;

8. The slab height is 150mm for GCCB1 and GCCB2 reference models, and 130mm for GCCB3, both with *Holorib* HR 51/150 geometry and support-to-support execution;

9. Steel S355 is adopted ( $f_y = 355$  MPa and  $f_u = 490$  MPa). The longitudinal elastic modulus is 200 GPa;

10. The average strength of concrete is 36.6 MPa for GCCB1 and GCCB2 references and 33 MPa for GCCB3.

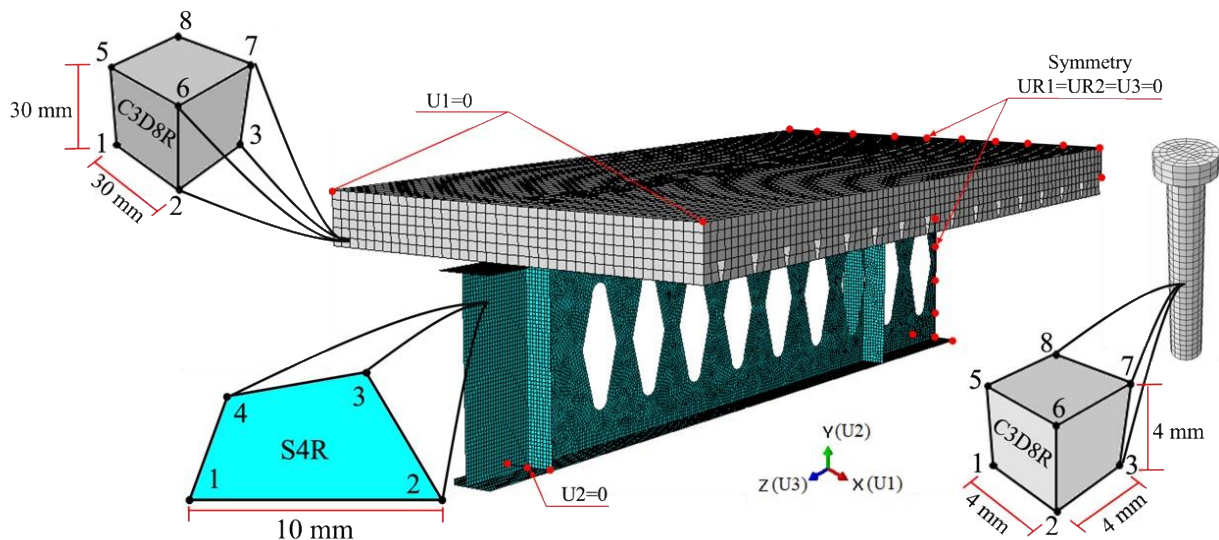
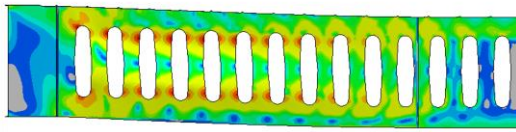
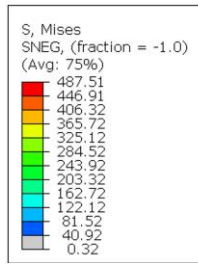


Figure 4: Boundary conditions and discretization, numerical steel concrete composite beams with elliptically-based web openings

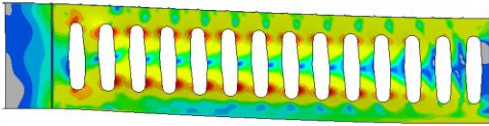
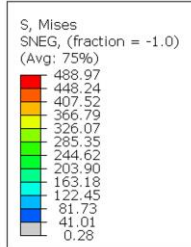
### 3 RESULTS AND DISCUSSIONS

Comparing the results obtained for models GCCB1, GCCB2 and GCCB3, it can be seen in Figure 5 that models GCCB1, GCCB2 and GCCB3 present a failure mode defined by web-post buckling (WPB) for models with small  $w/d_o$  ratios and  $R/d_o$ . On the other hand, as the  $w/d_o$  and  $R/d_o$  ratios increase, the GCCB2 and GCCB3 models begin to have failures governed by the Vierendeel mechanism (VM).

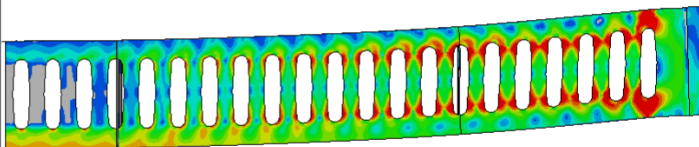
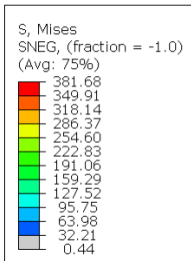
According to Figure 5, it can be seen that the increase in the width of the web post tends to cause a lower concentration of elongation in the web post element. This situation was observed mainly for models with  $w/d_o = 0.65$ , where there is the largest opening ratio and the largest widths of the web uprights. Even so, it is noted that models GCCB2 and GCCB3 tend to fail due to a plastic mechanism as the opening width increases. This must be the position of the stiffeners, the size of the span and the elevation of the forces in the lower region of the center of the structure's span.



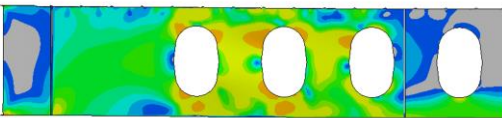
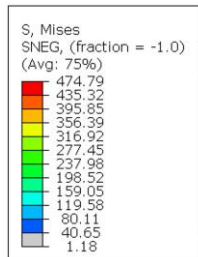
(a) Model GCCB1,  $w/d_o = 0,25$ ,  $R/d_o = 0,10$  and  $b_w/d_o = 0,20$



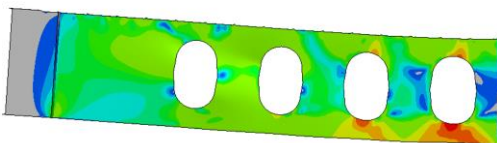
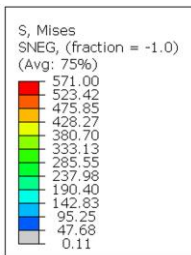
(b) Model GCCB2,  $w/d_o = 0,25$ ,  $R/d_o = 0,10$  and  $b_w/d_o = 0,20$



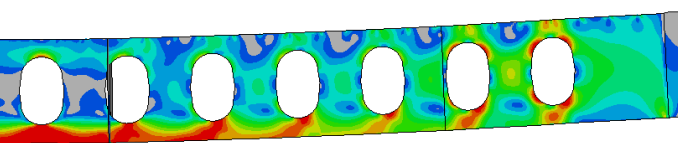
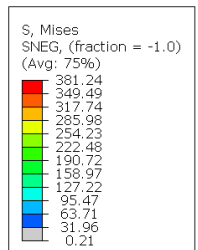
(c) Model GCCB3,  $w/d_o = 0,25$ ,  $R/d_o = 0,10$  and  $b_w/d_o = 0,20$



(d) Model GCCB1,  $w/d_o = 0,65$ ,  $R/d_o = 0,30$  and  $b_w/d_o = 0,60$



(e) Model GCCB2,  $w/d_o = 0,65$ ,  $R/d_o = 0,30$  and  $b_w/d_o = 0,60$



(f) Model GCCB3,  $w/d_o = 0,65$ ,  $R/d_o = 0,30$  and  $b_w/d_o = 0,60$

Figure 5: Failure modes (Von Mises stresses in MPa)

As shown in Figure 6, for the  $w/d_o$  curves under global shear force ( $V$ ) as a function of  $R/d_o$ , it is noticeable that the GCCB3 models have global shear values lower than the other reference models, regardless of the variation in the opening radius. For GCCB1 and GCCB2 models, when the ratios  $R/d_o$  are 0.10 and 0.15, the influence of the opening width occurs from the  $w/d_o$  ratio of 0.45. From this ratio onward, the global shear force becomes higher in the GCCB2 model. This can also be observed in the deformed configuration of the GCCB2 models, as from the  $w/d_o$  ratio of 0.45, the model switches its failure mode from WPB to VM. In the  $R/d_o$  ratios of 0.25-0.3, the global shear force in the GCCB2 model becomes consistently higher than the other models.

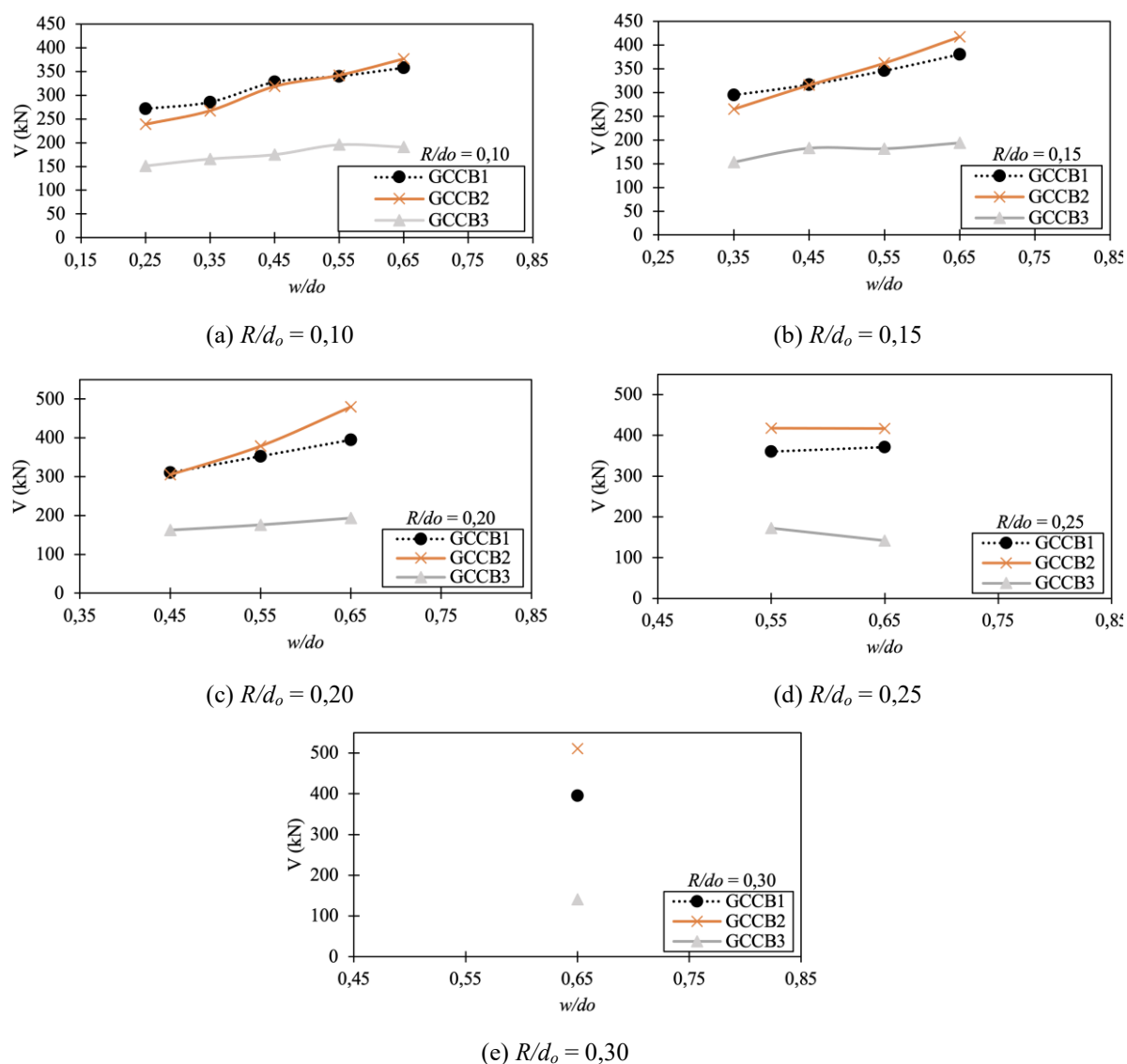


Figure 6: Comparison of elliptically-based parameters for GCCB1, GCCB2, and GCCB3, at a  $R/d_o$

For the  $b_w/d_o$  curves considering the overall shear effort, as a function of  $w/d_o$  from Figure 7, it is also observed that GCCB3 models have global shear ( $V$ ) values lower than other reference models regardless of the width of the web. As for GCCB1 and GCCB2 models, when the  $w/d_o$  ratios are between 0.25-0.45, the global shear effort for GCCB1 models is higher than that of the GCCB2 model. However, from the  $w/d_o$  ratio of 0.55 onwards, the influence of the opening width comes into play, and beyond this ratio, the global shear effort becomes greater in the GCCB2 model. This can be justified once again by the shift in the failure mode from

WPB to VM in the GCCB2 model, as higher  $w/d_o$  ratios, models with fewer openings and larger web width dimensions, tend to resist failure due to instability.

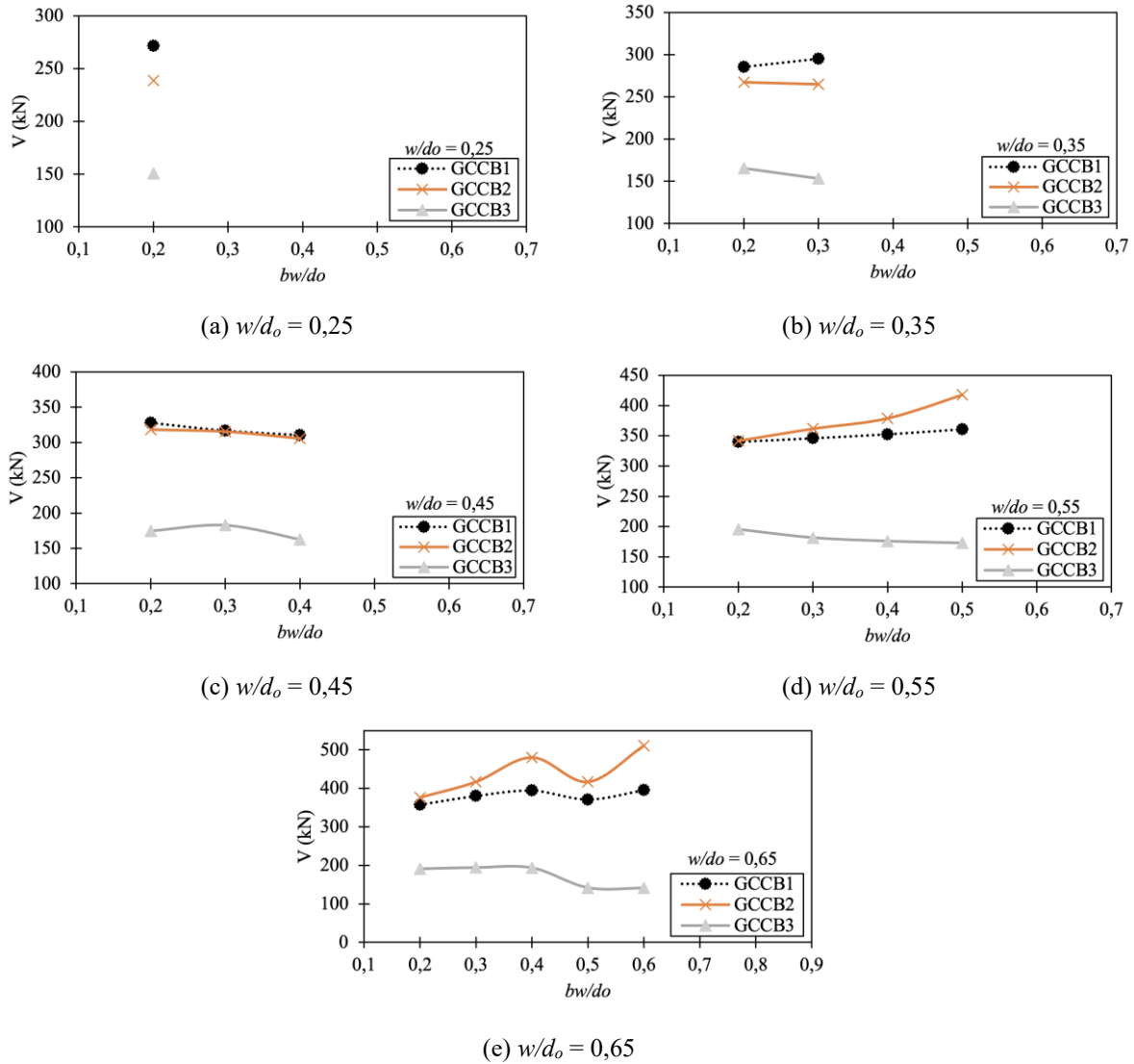


Figure 7: Comparison of elliptically-based parameters for GCCB1, GCCB2, and GCCB3, at a  $w/d_o$

#### 4 CONCLUSION

In this study, 45 models were developed for the parametric investigation. The GCCB1 models exhibit a failure mode characterized by web post buckling (WPB) instability. On the other hand, the GCCB2 and GCCB3 models show that the majority of failures are governed by the Vierendeel mechanism (VM). The parameters of opening radius and opening width tend to negatively influence the resistance capacity, while the width of the web post assists in resisting instability in the web post. It is noted that models with larger web post widths, in general, achieved higher resistance capacities. It is anticipated that the analysis of other  $d_o/H$  ratios for composite steel and concrete beams with elliptical base openings will provide further insights and understanding of these structures.

## 5 ACKNOWLEDGMENTS

This study was financed in part by the Centro Nacional de Desenvolvimento Científico e Tecnológico (CNPq), grant number #404719/2023-6, and Coordenação de Aperfeiçoamento de Pessoal de Nível Superior – Brasil (CAPES) – Finance Code 001.

## REFERENCES

- [1] Ferreira, F. P. V., Martins, C. H. and De Nardin, S., ‘Assessment of web post buckling resistance in steel-concrete composite cellular beams’, *Thin-Walled Structures*, v. 158, n. January, p. 106969, 2021.
- [2] Ferreira, F. P. V. *et al.*, ‘Steel-concrete-composite beams with precast hollow-core slabs: A sustainable solution’, *Sustainability (Switzerland)*, v. 13, n. 8, 2021.
- [3] Panedpojaman, P. W., Sae-Long; Chub-Uppakarn, T., ‘Cellular beam design for resistance to inelastic lateral – torsional buckling’, *Thin-Walled Structures*, v. 99, n. February 2016, p. 1–6, 2016.
- [4] Ellobody, E., ‘Nonlinear analysis of cellular steel beams under combined buckling modes’, *Thin-Walled Structures*, v. 52, n. March 2012, p. 66–79, 2012.
- [5] El-Sawy, K. M., Sweedan, A. M. I. and Martini, M. I., ‘Moment gradient factor of cellular steel beams under inelastic flexure’ *Journal of Constructional Steel Research*, v. 98, n. July 2014, p. 20–34, 2014.
- [6] Tsavdaridis, K. D. and D’mello, C., ‘Web buckling study of the behaviour and strength of perforated steel beams with different novel web opening shapes’, *Journal of Constructional Steel Research*, v. 67, n. 10, p. 1605–1620, 2011.
- [7] Tsavdaridis, K. D. and D’mello, C., *Structural Beam*, GB 2492176, 2012.
- [8] Tsavdaridis, K. D. and D’mello, C., ‘Optimisation of novel elliptically-based web opening shapes of perforated steel beams’, *Journal of Constructional Steel Research*, v. 76, n. September 2012, p. 39–53, 2012.
- [9] Ferreira, F. P. V. *et al.*, ‘EC3 design of web-post buckling resistance for perforated steel beams with elliptically-based web openings’, *Thin-Walled Structures*, v. 175, n. February, p. 109196, 2022.
- [10] Shamass, R. *et al.*, ‘Web-post buckling prediction resistance of steel beams with elliptically-based web openings using Artificial Neural Networks (ANN)’, *Thin-Walled Structures*, v. 180, n. August, p. 109959, 2022.
- [11] Ferreira, F. P. V. *et al.*, ‘Web-post buckling resistance calculation of perforated high-strength steel beams with elliptically-based web openings for EC3’, *Structures*, v. 55, n. May, p. 245–262, 2023.
- [12] EUROPEAN COMMITTEE FOR STANDARDIZATION. EN 1993-1-1: EUROCODE 3: Design of steel structures - Part 1-1: General rules and rules buildings. Brussels, 2005.
- [13] Panedpojaman, P., Thepchatri, T. and Limkatanyu, S., ‘Novel design equations for shear strength of local web-post buckling in cellular beams’, *Thin-Walled Structures*, v. 76, p. 92–104, 2014.
- [14] Yun, X., Gardner, L., ‘Stress-strain curves for hot-rolled steels’, *Journal of Constructional Steel Research*, v. 133, p. 36–46, 2017.
- [15] Araújo, D. De L. *et al.*, ‘Headed steel stud connectors for composite steel beams with precast hollow-core slabs with structural topping’, *Engineering Structures*, v. 107, p. 135–150, 2016.
- [16] CEB-FIP, FIB. Model Code 2010.
- [17] Hordijk, D. A., ‘Local approach to fatigue of concrete’, *Dissertation*, Delft University of Technology, 1991.
- [18] Ferreira, F. P. V., Rossi, A. and Martins, C. H., ‘Lateral-torsional buckling of cellular beams according to the possible updating of EC3’, *Journal of Constructional Steel Research*, v. 153, p. 222–242, 2019.

- [19] Nadjai, A. *et al.*, 'Performance of cellular composite floor beams at ambient temperature', *Fire Safety Journal*, v. 42, n. 6–7, p. 489–497, 2007.
- [20] Müller, C. *et al.*, 'Large web openings for service integration in composite floors', *Technical Steel Research*. European Commission, Contract No 7210-PR/315, v. Final repo, 2006.